A SURVEY OF THE KINEMATIC PROPERTIES OF GIANT EXTRAGALACTIC H II REGIONS

Héctor O. Castañeda, Casiana Muñoz–Tuñon

Instituto de Astrofísica de Canarias, 38200 La Laguna, Tenerife, Spain

Marcus V. F. Copetti

Universidade Federal de Santa Maria, Santa Maria, Brazil

and

Roberto J. Terlevich

Royal Greenwich Observatory, Madingley Road, Cambridge CB30EZ, UK

RESUMEN

Hemos utilizado TAURUS-2, un espectrógrafo Fabry-Perot en operación en el Observatorio del Roque de los Muchachos, para realizar el estudio de las propiedades cinemáticas del gas ionizado en una muestra de regiones H II gigantes cercanas. Discutimos en este artículo el procedimiento observacional, la reducción y análisis de los datos, y presentamos algunos de los resultados obtenidos durante nuestro trabajo.

ABSTRACT

The use of TAURUS-2 (a Fabry-Perot imaging spectrograph) for the study of the kinematics and the dynamics of giant extragalactic H II regions in nearby galaxies is discussed. The technical aspects of the instrument, together with the procedures adopted for data analysis and reduction, and some of the first scientific results of our program are also presented.

Key words: **ISM: KINEMATICS AND DYNAMICS — HII REGIONS**

1. INTRODUCTION

The study of the kinematics and dynamics of the ionized gas of Giant Extragalactic H II Regions (GEHRs) can provide us with information about the mechanisms which trigger star formation in those complexes, as well as the process related to the interaction between the clusters of massive stars and the gas. The gas is in a state of supersonic turbulence, as seen by the observed supersonic line widths of the emission lines (Smith & Weedman 1970), a phenomena that requires a source to continuously replenish the energy lost due to shocks. Two other significant properties associated to the kinematics of the gas are the clear correlation between luminosity, velocity dispersion, sizes and chemical abundances deduced from the integrated spectra (Melnick et al 1987; Hippelein 1986; Roy, Arsenault, & Joncas 1986) and the very high velocity gas at low surface brightness that it is observed in some nebulae, probably originated by supernova explosions or by stellar winds of massive stars (Chu & Kennicutt 1986; Castañeda, Vílchez, & Copetti 1990).

Most of the kinematic data in the literature comes from the integrated spectra of the nebulae, and relatively few studies have been done with high spatial and spectral resolution. Techniques of long-slit or echelle spectroscopy only allow partial spatial coverage of the object and are very telescope-time consuming, but nevertheless they have a large spectral coverage and, if the sampling is good, they allow for intercalibration of the zones not observed. An alternative approach is the use of Fabry-Perot spectroscopy due to its good spatial coverage, speed, and high spectral resolution. Imaging spectroscopy allows us to visually link changes in the kinematic parameters (velocity and σ) with spatial features of the region (ionizing clusters, shells, etc.).

267

The development in the last decade of a new generation of imaging spectrographs provide us with an excellent tool for the study of the kinematics of GEHRs.

With the aim of solving some of the most important problems related to the gas dynamics in GEHRs, we have used TAURUS-2, a Fabry-Perot spectrograph at the Observatorio del Roque de Los Muchachos to obtain spectra with high spatial resolution for a large sample that represents a wide range of different type of objects, including classical, high surface brightness, diffuse, multiple core, shell, and supergiant objects. In this short article we discuss some of the results of our work.

2. OBSERVATIONS

Imaging spectroscopy in Hα and [O III] λ5007 lines was carried out for the main regions of M101, M33, NGC 2403, NGC 2366 and NGC 6822, during two runs in July 1990 and January 1991. TAURUS-2 (Atherton & Taylor 1980) was used with a photon-counting device (IPCS-II) as detector, together with a Queensgate (125 microns gap) etalon. The format of the data cube was 256×256 in the spatial scale ($0.26''$ pixel^{-1}), and 100 planes (steps) in the wavelength dimension, with typical integration times of one hour. A fast scan was completed over 10% of the free spectral range, to have two complete sets of rings and estimate the main parameters of the etalon via the calibration data cube. A top flat interference filter at or near the appropriate redshift of each object was used to isolate a single order of interference. A calibration cube was obtained at the beginning of the night, and later used to obtain the free spectral range and to compute the etalon gap. To monitor any mechanical deformations of the etalon and to check its optical stability, a calibration ring was obtained at the beginning and end of each observation.

3. DATA REDUCTION

After the data is phase corrected the final result is a calibrated data cube in which the third coordinate is the wavelength. A program can be used to automatically fit Gaussians to the spectrum associated with each point, within square areas defined by boxes of arbitrary size (Lewis & Unger 1992). Only a fraction of the data is true emission from the object, and a mask can be used to fit the areas with meaningful signal. Further analysis of the data introduces the rejection of points of fits, based on criteria such as low signal to noise, unphysical line width, etc. The final results are maps that reflect the different kinematic properties of the ionized medium such as the radial velocity and line width (σ),
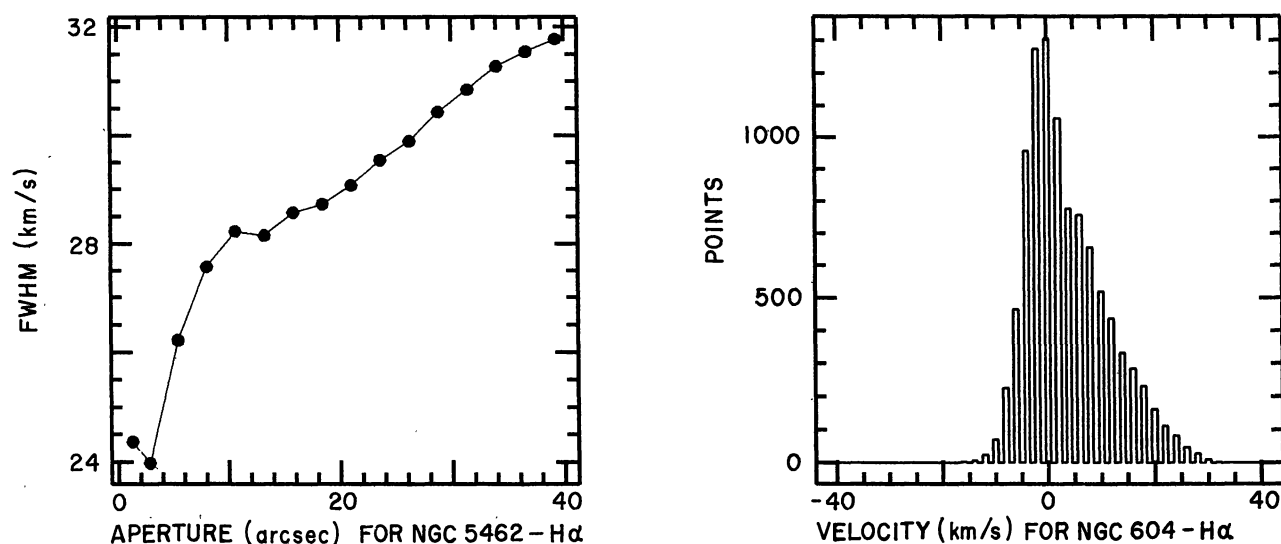

Fig. 1. (*Left*) Synthetic aperture analysis for NGC 5462. (*Right*) Velocity histogram for NGC 604.

4. ANALYSIS OF THE DATA

Three-dimensional spectroscopic data make it possible to select among strategies for the study of the kinematic properties of the objects. For example, *aperture analysis* (to obtain synthetic spectra at different apertures to simulate integrated spectra with different diaphragms) is useful to establish if the emission line profiles used to measure the velocity dispersion are representative of the whole region. The data cube allows us to do synthetic aperture analysis with square apertures of arbitrary size. It is then possible to compare the contributions to the integrated spectra from different parts of the nebulae. This approach is very useful to determine if the integrated line spectra reflect the total kinematics of the nebula or the velocity dispersion of particular positions (for example, the brightest knots). In Figure 1 (Left), we show the value of σ (before correction for instrumental line width) obtained with synthetic aperture spectroscopy in Hα for the region NGC 5462 in M101, measured from the point of the complex with highest surface brightness. We see that the velocity dispersion from the integrated spectra depends on the aperture selected. A different behavior is observed in other nebulae, for example NGC 604 (see below).

Velocity histograms are very important for the study of large scale motions within the regions that influence the emission line profile. Such large scale motions in the complex may arise from collapse or expansion of the region, as well as from galactic motions (shear and rotation). The histograms can be characterized by their statistical asymmetry parameters. It is interesting to note that systematic motions in the form of velocity gradients with a well defined pattern have, in fact, been observed, and confirmed by comparison of velocity maps in different emission lines. An example is illustrated in Figure 1 (Right), where we show the velocity histogram for NGC 604, with the zero point in velocity selected at the position of the brightest knot.

5. SOME RESULTS

The combined use of *intensity, velocity, and velocity dispersion maps*, together with the study of *individual spectra* at selected points have been used to characterize the kinematics of selected regions. Here we mention some of the results obtained for the largest complexes in M101, M33, and NGC 2366.

A study of NGC 5471, the brightest H II complex in M101, has been made by Muñoz–Tuñon (1994). The object has five condensations ("knots") surrounded by a diffuse gas envelope, with an angular size of $\sim 16''$. The study of the line width shows that all the emission profiles from the sampled area are supersonic, with a large fraction ($\sim 80\%$) of the emitting area presenting a roughly constant emission-line width with Gaussian profiles characterized by $\sigma \sim 20$ km s^{-1}. Splitting of the lines has been detected in a small area of the border of the nebula.

The largest H II complex in M33, NGC 604, was the subject of the Ph.D. thesis of N. Sabalisck (1995; see also Sabalisck et al. 1995). Shells, filaments, and loops are clearly distributed in the low surface brightness halo, while two main emitting knots dominate the emission. These knots are responsible for the observed global velocity dispersion value: the line profiles that arise from the highest intensity regions of NGC 604 show well-defined Gaussian profiles with an intrinsic supersonic velocity dispersion of 16.5 km s^{-1} in Hα, the same order as the supersonic global velocity dispersion associated with NGC 604. The largest values of σ (> 20 km s^{-1}) are found in zones of low intensity which present line profiles with strong asymmetries or splitting. These lines are most likely due to the action of many strong stellar winds caused by the massive stars in the region which are presently disrupting large sections of the original parent cloud.

The most peculiar region in the sample is NGC 2363, the largest H II region in the irregular galaxy NGC 2366. Roy et al. (1991) found line splitting in the [O III] line, which they attributed to a bubble with a diameter of 200 pc, at an expansion velocity of 45 km s^{-1}. We observed the object in Hα and [O III]. The [O III] line is split, with a maximum separation between the two components of ~ 80 km s^{-1}. The emission in Hα, on the contrary, does not show any anomaly in the line profile.

Fabry-Perot spectrometry allows to exam the velocity field at each plane of the data cube, which is very useful in order to visualize peculiar features of the velocity field. In Figure 2 we show the isocontours of the image produced by the collapse in the spectral direction of the data cube in [O III], as well as a partial collapse (2 planes = 15 km s^{-1}) centered on the plane where the global [O III] line is centered. From the figure it can be seen that the bubble is asymmetric (6.4$''$ E–W, 5.9$''$ N–W), but its dimensions are smaller than those reported by Roy et al. The discrepancy can be attributed to the the lower integration time (3 600 s of us vs. 30 000 s of Roy et al.), and the smaller resolution power of our data, which does not allow us to observe the line splitting in the periphery. The geometrical center of the shell is not coincident with the brightest knot of the region, and is displaced with respect to the excess of emission at $\lambda 4686$ found by Drissen, Roy, & Moffat (1993), which they attribute to stellar lines of Wolf-Rayet stars.
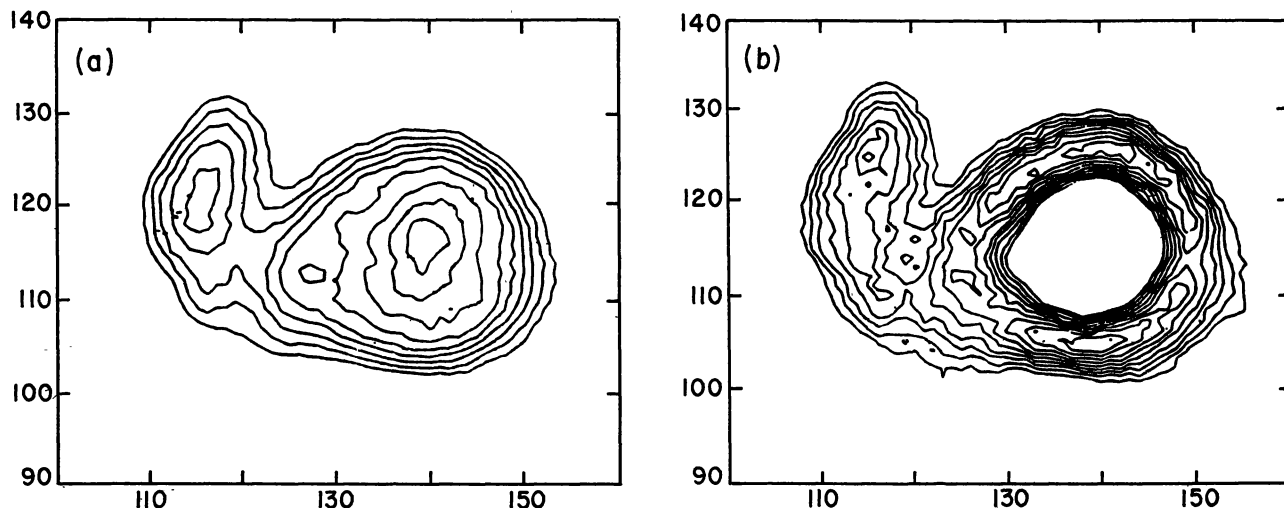
Fig. 2. (a) [O III] isocontours for NGC 2363 from the collapse of the data cube in the spectral direction. (b) Collapse of the planes (53,54) equivalent to a velocity interval of 15 km s^{-1}. North is up, East is left; 1 pixel = 0.26" (from Castañeda 1994).

REFERENCES

Atherton, P. D., & Taylor, K. 1980, MNRAS, 191, 675
Castañeda, H. O., Vílchez, J. M., & Copetti, M. V. F. 1990, ApJ, 365, 164
Castañeda, H. O. 1994, in IAU Colloquium 149, Tridimensional Optical Spectroscopic Methods in Astrophysics, ed. G. Comte & M. Marcelin (San Francisco: ASP Conf. Ser.), 138
Chu, Y.-H., & Kennicutt, R. C. 1986, ApJ, 311, 85
Drissen, L., Roy, J.-R., Moffat, A. F. J. 1993, AJ, 106, 1460
Hippelein, H. 1986, A&A, 160, 374.
Lewis, J. R,. & Unger, S. 1992, in Astronomical Data Analysis and Systems 1, ed. D. M. Worral, C. Biemesderfer & J. Barnes (San Francisco: ASP Conf. Ser.), 445
Melnick, J., Moles, M., Terlevich, R., & García–Pelayo, J. 1987, MNRAS, 226, 849
Muñoz-Tuñón, C. 1994, in Violent Star Formation from 30 Doradus to QSOs, ed. G. Tenorio-Tagle (Cambridge: Cambridge Univ. Press), 25
Roy, J.-R., Arsenault, R., & Joncas, G. 1986, AJ, 300, 624
Roy, J.-R., Boulesteix, J., Joncas, G., & Grundseth, B. 1991, ApJ, 367, 141
Sabalisck, N. S. P 1995, Ph.D. thesis. Univ. de Sao Paulo, Brasil
Sabalisck, N. S. P., Tenorio-Tagle, G., Castañeda, H. O., & Muñoz–Tuñon, C. 1995, ApJ, 444, 200
Smith, M. G., & Weedman, D. 1970, ApJ, 161, 33
—————. 1972, ApJ, 172, 307